63-4-1

7

RESEARCH REPORT EE 544

INVESTIGATION OF THE EFFECTS OF DRIVING THE MIDDLE CAVITY OF A THREE-CAVITY KLYSTRON

D. Reynolds

Interim Report

15 October 1962

School of Electrical Engineering
CORNELL UNIVERSITY
Ithaca, New York

RESEARCH REPORT EE 544

INVESTIGATION OF THE EFFECTS OF DRIVING THE MIDDLE CAVITY OF A THREE-CAVITY KLYSTRON

D. Reynolds

LINEAR BEAM MICROWAVE TUBES

Interim Report 15 October 1962

Published under Contract No. AF30(602)-2573
Rome Air Development Center, Griffiss Air Force Base, New York

CONTENTS

LIST OF SYMBOLS

$-\lvert I_o \rvert$	=	average current density in beam
i	=	a-c current density at location z
i_1	=	a-c current density at the end of the first drift space
i_3	=	a-c current density entering the third gap
i_{tot}	=	total current density = $-\lvert I_o \rvert + i$
V_o	=	d-c beam voltage
V_1	=	a-c voltage across the first gap with a positive sign producing a net acceleration of an electron
V_2	=	a-c voltage across the second gap with a positive sign producing a net acceleration of an electron
V_{21}	=	portion of a-c voltage across the second gap resulting from beam current
V_{22}	=	portion of a-c voltage across the second gap resulting from external drive at the middle cavity
u_o	=	average beam velocity
u	=	a-c beam velocity at point z
u_1	=	beam velocity at the end of the first drift space
u_{exit}	=	beam velocity at the exit from the second gap
u_3	=	a-c beam velocity entering the third gap
u_{10}	=	magnitude of velocity modulation impressed upon beam by the first gap
P_1	=	power input to first cavity
P_2	=	power input to second cavity
P_3	=	power output from third cavity
Z_c	=	magnitude of impedance of middle cavity as seen by the beam
ϕ	=	impedance angle of middle cavity as seen by beam

θ_1 = d-c transit angle of the first gap

θ_2 = d-c transit angle of the second gap

θ_d = d-c transit angle of the second drift space

M_1 = gap-coupling coefficient of the first gap = $\sin \frac{\theta_1}{2} \Big/ \frac{\theta_1}{2}$

M_2 = gap-coupling coefficient of the second gap = $\sin \frac{\theta_2}{2} \Big/ \frac{\theta_2}{2}$

ω = operating angular frequency

ω_p = plasma resonant frequency

β_e = electronic propagation constant = ω/u_o

β_p = plasma propagation constant = ω_p/u_o

ρ = beam total charge density = $-|\rho_o| + \rho_1$

$-|\rho_o|$ = average charge density in beam

ρ_1 = a-c charge density in beam

d_1 = spacing of first gap

d_2 = spacing of second gap

d_3 = spacing of third gap

S_1 = length of first drift space

S_2 = length of second drift space

ABSTRACT

This report describes an experimental and theoretical investigation of the effects of driving the middle cavity of a three-cavity klystron. It indicates that drive power levels within a few decibels of the power output of the tube increase the total power output or efficiency no more than proper tuning of the middle cavity. Included are preliminary results of a theoretical study based upon a combination of space-charge waves and first-order ballistic theory.

INTRODUCTION

In the course of development work that resulted in the multiple-beam klystron, Dehn[1] applied power to the middle cavity of a three-cavity klystron and observed that, under some conditions, he obtained an increase in output power of 100w when he applied 100w to the middle cavity. When losses in coupling and in the cavity itself were taken into account, this meant that a power gain was achieved, which could conceivably result in a higher total efficiency for the tube. It was decided to investigate this effect at Cornell to see if it could be reproduced, increased, and explained theoretically.

The original plan was to carry out experimental work on the SAL-36 klystron, a three-cavity klystron rated at a nominal beam voltage of 160 kv peak, with a cathode perveance of one microperv,* and an operating frequency of 840 Mc/s. It was planned to use a relatively high-power traveling-wave tube as a driver for measurements at low power levels and to apply output power from the SAL-36 through a power divider for measurements at higher power levels. Because of experimental difficulties with the SAL-36 system, it was necessary to make measurements on the SAS-61 klystron, a three-cavity klystron operating at S-band (2700-2900 Mc/s). The SAS-61 has a cathode perveance of three micropervs and is designed to operate at a beam voltage of 13 kv with a maximum pulse width of 10 μsec. A major advantage of using this system lay in the possibility of attaining input power levels of the order of the output power of the tube under test by using a sec-

*One microperv $= \left(\frac{\text{amperes}}{\text{volts}^{3/2}}\right) \times 10^{6}$

ond SAS-61** tube as a driver. A further advantage was the availability of a wider range of auxiliary equipment at this frequency range.

EXPERIMENTAL RESULTS

The initial portion of the work reported here consisted of an experimental investigation into the effects of driving the middle cavity of a SAS-61 klystron. It was first planned to vary the relative phase of the drive at the middle cavity with respect to that at the first cavity over increments of 30 degrees in phase. It was soon apparent that most of the changes observed were of the order of the experimental error, except at those points where the relative phase was such as to produce minimum output, where a noticeable reduction in output power occurred. Data were therefore obtained at the condition of middle-cavity drive power giving minimum output, and at a point 180 degrees removed in phase from this point.

It was also planned in the beginning to observe the effects of varying levels of middle-cavity drive power. Early observations showed, however, that the output power varied linearly with changes in middle-cavity drive power. Points were therefore taken only for an applied middle-cavity drive power of 1 kw.

Experimental data were obtained on equipment connected as shown in Figure 1. A single modulator was used to drive both the driver tube and the tube under test. It was necessary to operate the modulator at 60 cps to minimize pulse amplitude jitter resulting from voltage variations among

**This was made possible through the kind co-operation of Dr. A. D. Sutherland of the Sperry Gyroscope Company, Gainesville, Florida, who arranged to have a SAS-61 tube donated for the purposes of this experiment.

phases of the supply. R-F drive power was obtained from a reflex klystron and amplified to an appropriate level by a traveling-wave amplifier. This signal was applied to the input cavity of the driver klystron, whose output was split to provide drives for both the first and second cavities of the tube under test. Two attenuators and a coaxial trombone provided virtually independent control of signal amplitude and relative phase.

Various directional couplers were connected as indicated in Figure 1 to allow measurement of forward and reflected power at all three cavities of the tube under test. An additional directional coupler was inserted in the input to the first cavity of the tube under test to provide a phase reference signal. A slotted line in the input to the middle cavity allowed selection of a comparison signal for determination of relative signal phase. The slotted line was equipped with a r-f adaptor instead of the usual crystal. Its output was combined with the output taken by directional coupler in the feed to the first cavity. The combination was mixed with a local-oscillator signal, and the detected output was amplified and displayed on an oscilloscope. A phase difference introduced by changing the length of the trombone could be measured by the shift in position of the slotted-line carriage necessary to obtain a null indication. This technique was described fully in an earlier report.[2]

Since the SAS-61 klystron is designed for pulse operation, it was necessary to measure peak power. This was accomplished by placing a calibrated attenuator before a crystal and displaying the crystal output on an oscilloscope. An absolute reading was obtained by comparing the reading from this device with that from a power bridge on the c-w r-f output of the traveling-wave tube. The change in attenuation necessary to reach the same voltage level on the oscilloscope display was a measure of the change in

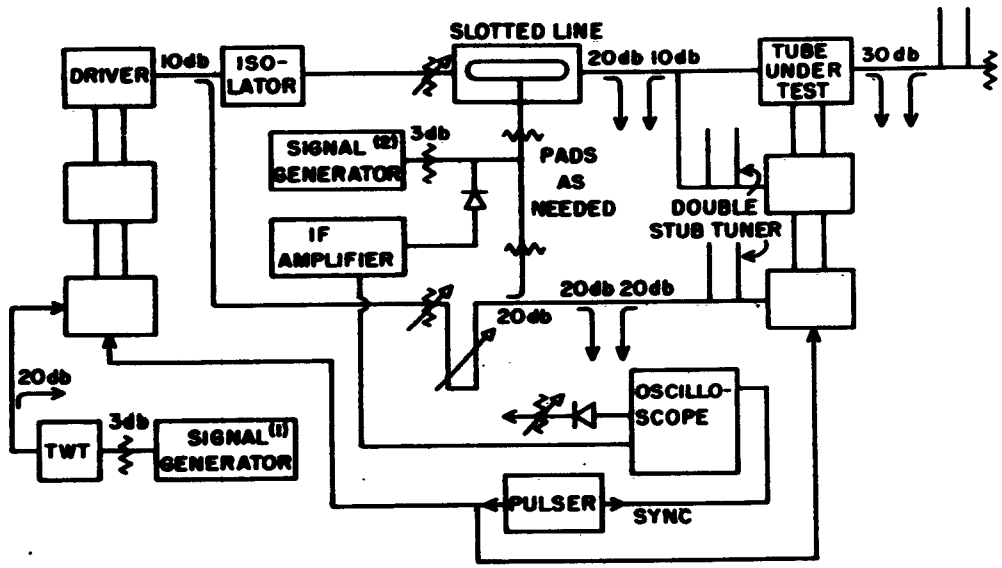

Driver and Tube under Test - Sperry SAS-61 three-cavity klystrons. 2700-2900 Mc/s, nominal operating voltage 13kv, maximum pulse length 10μsec.

Isolator - Ferrite, cascade model

Signal Generator - (1) Sperry Microline using a 417-A reflex klystron (2) Polarad Microwave (S-band)

TWT - RCA 4010 traveling-wave tube

I-F Amplifier - General Radio Unit

Slotted Line - Hewlett-Packard 810A

Oscilloscope - Tektronix 585 with high-gain preamplifier

Pulser - Capable of supplying d-c to tube heaters and variable pulses synchronized to line frequency with peak voltages to 20kv, variable pulse width.

Note - Numbers indicate magnitude of fixed attenuators or of the coupling ratio for directional couplers.

Figure 1. Modified Block Diagram of Test Equipment for Investigating Effects of Middle-Cavity Drive.

power level of the unknown signal from the reference level.

The large number of cascaded voltage-sensitive elements of the experimental circuit resulted in excessive sensitivity to small variations in line voltage. A series line-voltage regulator solved this problem for all equipment except the modulator, which required three-phase power. Variation in the pulse amplitude of the modulator was finally controlled by installing a differential amplifier to control bias on the charging tetrode according to an error signal produced by comparing a portion of the output signal with the voltage across a gas voltage-regulator tube. Before the addition of the differential-amplifier circuit, pulse voltage on the driver and on the tube under test was observed to vary more than 500 v with normal line-voltage ripple. After the change, the variations were observed to be less than one per cent.

In addition to measurements of power inputs and outputs and of relative phase, various incidental measurements were necessary. These included a check on the perveance of the tube under test and information sufficient to determine cavity Q's under the effects of beam loading. Voltage points for determining perveance were obtained from oscilloscope measurements of pulse voltage with a viewing resistor, and current points were calculated from the duty cycle and the indicated average current. The duty cycle was set at 6×10^{-4} through the use of a line-synchronized 60-cps repetition rate and the maintenance of a 10-μs pulse width. Pulse width was set by adjusting first-cavity drive power to give a desired peak output power and then adjusting pulse width to provide the corresponding reading of average power on a power bridge.

Information sufficient to determine cavity Q's was obtained by using reversed directional couplers and measuring direct and reflected power with

the device described for measuring peak power. The conventional methods of making this determination were not possible because it was necessary to make measurements only when the pulse was on.

It can be seen from Figure 1 that a double-stub tuner was placed at the input to the middle cavity. This was necessary because in the SAS-61 the input loop at the middle cavity is intended as a sampling loop only, and is highly undercoupled as would be expected. The double-stub tuner was inserted to provide the best possible match to the middle cavity. All determinations of middle-cavity drive power were made with this tuner adjusted to minimize reflected power.

Figures 2 through 6 show power output plotted as a function of first-cavity drive power for middle-cavity drive power at zero, at 1 kw in the most favorable phase, and at 1 kw in the most unfavorable phase. The parameter

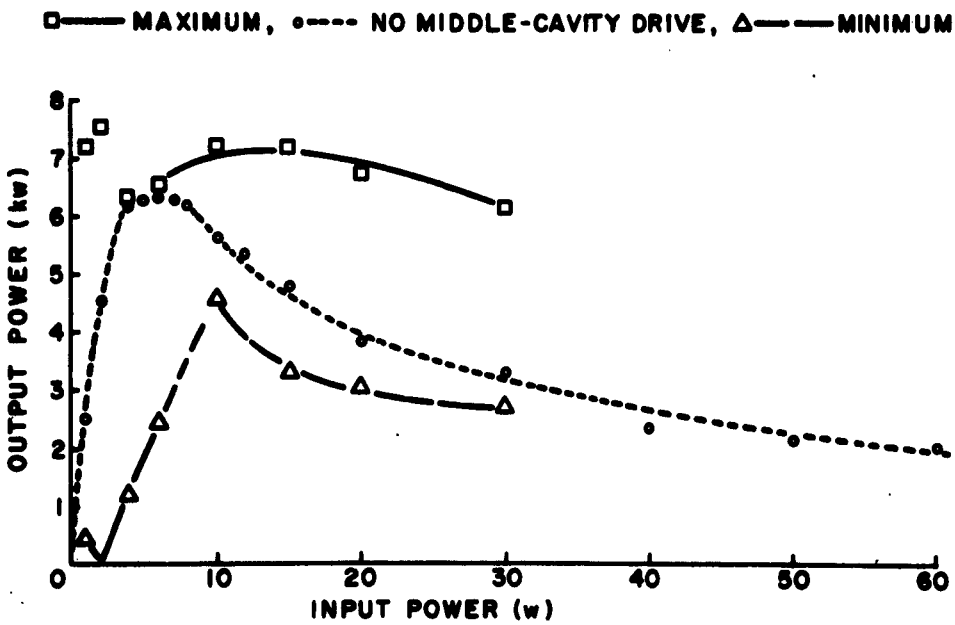

Figure 2. Gain Curve of SAS-61 Klystron with Middle Cavity Tuned for Maximum No-Drive Output at 200 mw (Synchronous); 1 kw to Middle Cavity.

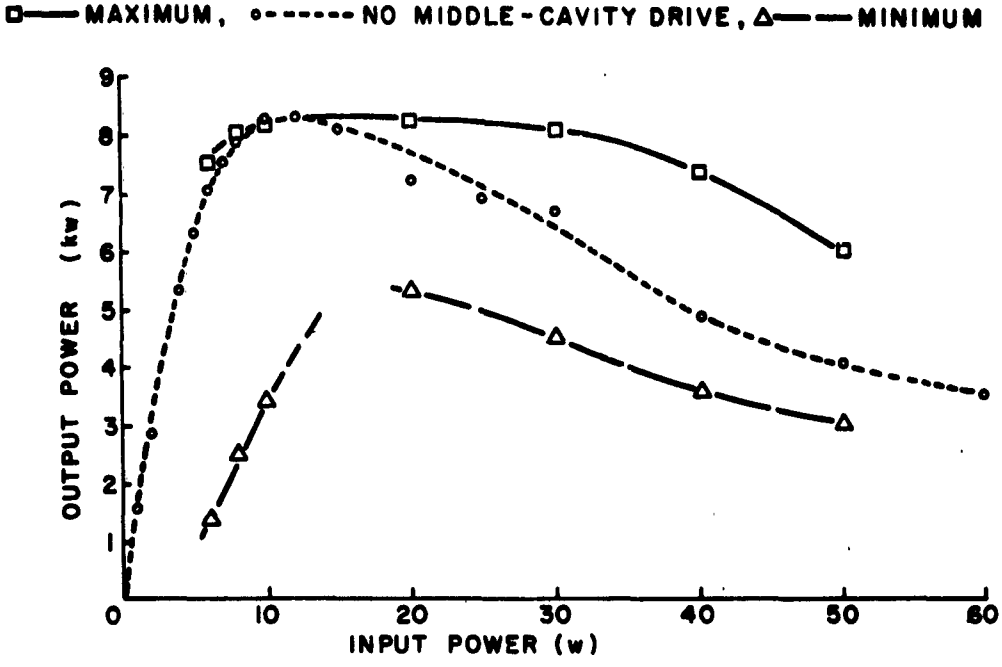

Figure 3. Gain Curve of SAS-61 Klystron with Middle Cavity Tuned for Maximum No-Drive Output at 10-w Drive; 1 kw to Middle Cavity.

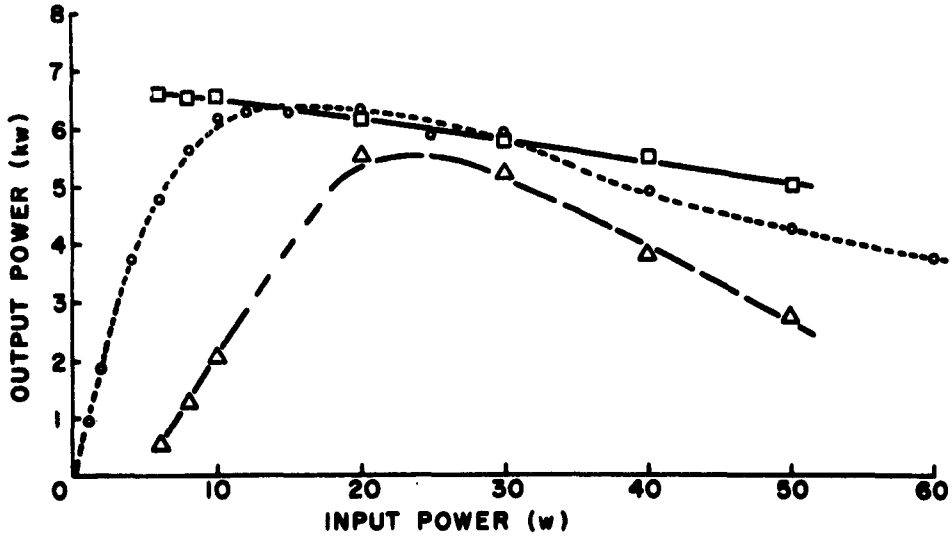

Figure 4. Gain Curve of SAS-61 Klystron with Middle Cavity Tuned for Maximum No-Drive Output at 20-w Drive; 1 kw to Middle Cavity.

□——MAXIMUM, o------NO MIDDLE-CAVITY DRIVE, Δ— — —MINIMUM

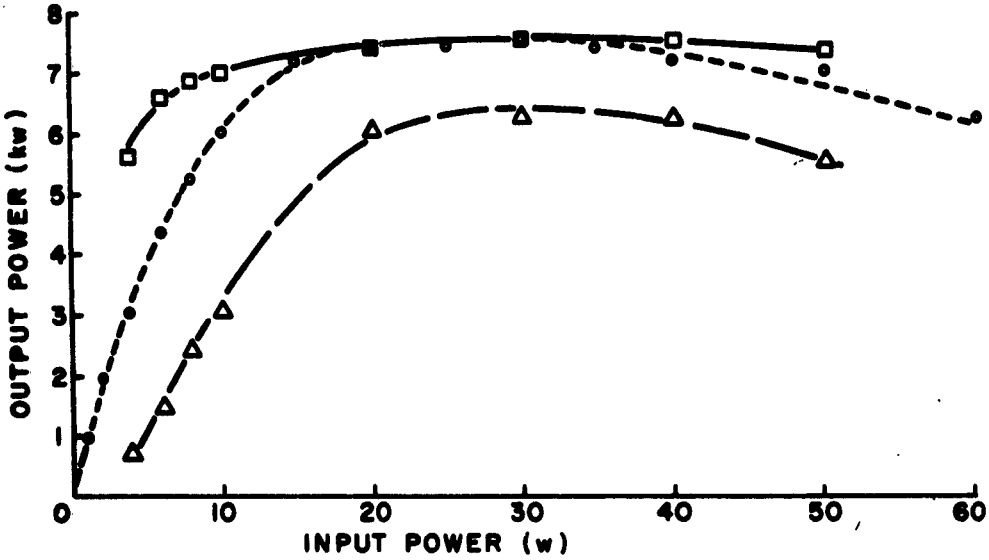

Figure 5. Gain Curve of SAS-61 Klystron with Middle Cavity Tuned for Maximum No-Drive Output at 30-w Drive; 1 kw to Middle Cavity.

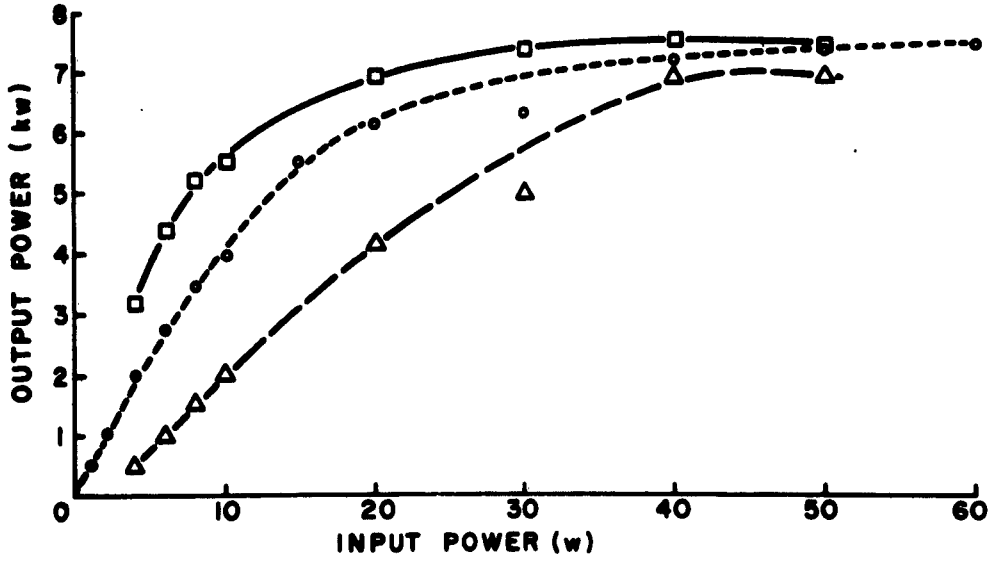

Figure 6. Gain Curve of SAS-61 Klystron with Middle Cavity Tuned for Maximum No-Drive Output at 50-w Drive; 1 kw to Middle Cavity.

is middle-cavity tuning. It will be seen that the effect of driving the middle cavity in favorable phase is to increase the output power whenever the middle cavity is tuned below the frequency at which output power is optimum at that particular level of first-cavity drive power. At no time, however, is the increase greater than the amount which could be obtained at the same drive level by optimum tuning of the middle cavity. Furthermore, the increase in power output over the no-drive case disappears as first-cavity drive power is reduced to the level where maximum output power occurs. At this drive level the effect of middle-cavity drive is apparent only in the unfavorable phase, when it has the effect of reducing output power.

A review of the parameters of the experiment seems in order. Synchronously tuned, the SAS-61 klystron used in this study had a maximum power output of 7.2 kw with 5 w drive at the first cavity and no power applied to the middle cavity. The tube was rated for a maximum power input of 30 w. Measurements were made with peak input powers into the first cavity of up to 100 w, and with the middle cavity up-tuned for maximum output at 10 w, 20 w, 30 w, and 50 w. Observations were also made of the behavior of the tube with middle-cavity drive when the drive at the first cavity was below saturation as the cavity was then tuned. Under these conditions the power output leveled off, and the behavior of the tube can best be described as that of a two-cavity klystron with its gain increased slightly by the initial modulation impressed upon the beam by the first cavity.

THEORETICAL STUDY

The SAS-61 tube has an oxide-coated unipotential cathode, gridded gaps, and an electron beam focused by space charge. There is no magnetic

focusing, and the tube is designed for pulse operation at a maximum pulse width of 10 μsec. Since the nominal perveance of this tube is relatively high, there is a considerable space-charge debunching resulting in variation of the beam diameter as the beam passes from the cathode to the anode. The tuning of the three cavities is accomplished by decreasing their longitudinal dimensions, which thus has the effect of changing the length of the gap when the cavity is tuned. It is necessary, therefore, to introduce some radical simplifying assumptions in arriving at a mathematical model that will enable prediction of the response of the device to middle-cavity drive power.

The model chosen to represent the SAS-61 klystron is a three-gap structure through which an infinitely wide electron beam is passed. A sinusoidal voltage pplied across the first gap produces space-charge waves in the first drift space. This results in a set of input conditions of velocity and a-c current at the second gap. Voltage across the second gap is produced both by the input a-c beam current and by external drive power at the middle cavity. The total second-gap voltage is combined with second-gap input conditions to determine the exit velocity from the gap. The beam is then considered to behave ballistically in the second drift space. Standard ballistic analysis[3] is used to determine a-c current in the final gap, and thus, to determine output power from the third gap. Thus, the justification of the assumption of linear space-charge waves in the first drift space is based upon the observations shown in Figure 7. For a range of input powers exceeding those used in experimental measurements, the two-cavity klystron consisting of the first cavity, first drift space, and the second cavity performs as a linear amplifier. This model does not represent a three-cavity klystron over a wide range of variations of a_1, the normalized first-cavity voltage;

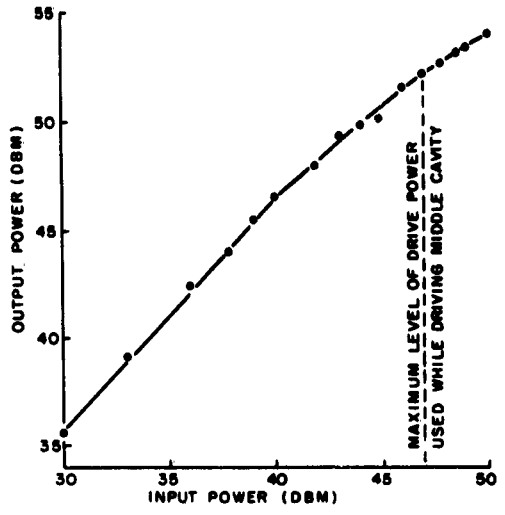

Figure 7. Input Power Gain of SAS-61 Using First and Second Cavities as a Two-Cavity Klystron.

but over the range of operation of this klystron, the first drift space is essentially linear. This is believed to be a valid approximation to the conditions of operation of the typical multiple-cavity klystron. It is emphasized, though, that this condition will not in general be true for a structure in which a_1 varies over a wide range.

The space-charge-wave analysis of the first drift space begins with Maxwell's curl equations, Newton's second law, and the assumption of waves of form $e^{j(\omega t-\gamma z)}$ in a vacuum;

$$\nabla \times \bar{H} = \bar{J} + \frac{\partial \bar{D}}{\partial t} = \bar{J} + \epsilon_o \frac{\partial \bar{E}}{\partial t} , \qquad (1)$$

$$\nabla \times \bar{E} = -\frac{\partial \bar{B}}{\partial t} = -\mu_o \frac{\partial \bar{H}}{\partial t} , \qquad (2)$$

$$m \frac{d}{dt} \bar{u} = -|e| \bar{E} . \qquad (3)$$

It is further assumed that a-c cross products of charge density and velocity are sufficiently small to be neglected, so that

$$\overline{I} = \rho\overline{u} - I_o = -|\rho_o|\overline{u} + \rho_1\overline{u}_o \quad . \tag{4}$$

The Eulerian total time derivative, together with the assumption that the a-c velocity is small compared with the total velocity, results in

$$\frac{d}{dt} = \frac{\partial}{\partial t} + u_{tot}\frac{\partial}{\partial z} \approx j\omega - j\gamma u_o \quad , \tag{5}$$

$$m\left[j\omega - j\gamma u_o\right]\overline{u} = -|e|\overline{E} \quad . \tag{6}$$

The assumption of motion in the z-direction only, i.e., absence of transverse motion, reduces Equation (6) to

$$u = -j\frac{e}{m}\frac{Ez}{u_o}\frac{1}{(\gamma-\beta_e)} \quad . \tag{7}$$

Applying the equation of continuity of charge, and using the resulting statement for a-c current in Equation (4), gives

$$\nabla\cdot i + \frac{\partial\rho}{\partial t} = 0 \quad , \tag{8}$$

where

$$\rho = \frac{\gamma}{\omega} i \quad ;$$

$$i = -|\rho_o|u + \frac{\gamma}{\omega} i u_o = -\frac{|\rho_o|\beta_e u}{(\gamma-\beta_e)} \quad , \tag{9}$$

Or, upon substituting the value of u from Equation (7),

$$i = \frac{-j\omega\epsilon_o\beta_\rho^2 E_z}{(\gamma-\beta_e)^2} \quad . \tag{10}$$

Equations (7) and (10) now lend themselves to application to a klystron drift space through the application of the following initial conditions:

$$i_x = 0 = i_y \, , \quad \frac{\partial}{\partial x} = 0 = \frac{\partial}{\partial y} \, , \quad i = i_z \quad . \tag{11}$$

Combination of Equation (1) and the initial conditions (11) leads to

$$i_z + j\omega\epsilon_o E_z = 0 \quad . \tag{12}$$

Substitution of Equation (12) into Equation (10) leads to

$$-j\omega\epsilon_o E_z = \frac{-j\omega\epsilon_o\beta_\rho^2 E_z}{(\gamma-\beta_e)^2} \; ; \quad \gamma = \beta_e \pm \beta_\rho \quad . \tag{13}$$

When an electric field is assumed, which can be described by

$$E_z = Ae^{j(\omega t - \gamma_1 z)} + Be^{j(\omega t - \gamma_2 z)} \, , \tag{14}$$

and the effect of the first cavity of the model is treated as a velocity jump equal in magnitude to $u_{10}e^{j\omega t}$, one can apply the initial condition,

$$i = 0 \quad \text{when} \quad z = 0 \, , \tag{15}$$

and evaluate and substitute constants A and B to give

$$E_z = u_{10} \frac{m}{e} u_o \beta_\rho \sin(\beta_\rho z)\, e^{j(\omega t - \beta_e z)}, \tag{16}$$

$$i = -j \frac{\beta_e}{\beta_\rho} |I_o| \frac{u_{10}}{u_o} \sin(\beta_\rho z)\, e^{j(\omega t - \beta_e z)}, \tag{17}$$

$$u = u_{10} \cos \beta_\rho z\, e^{j(\omega t - \beta_e z)}. \tag{18}$$

The initial conditions at the second gap of the model result from the substitution of the length S_1 of the first drift space for z, as follows:

$$i = -j \frac{\beta_e}{\beta_\rho} |I_o| \frac{u_{10}}{u_o} \sin(\beta_\rho S_1)\, e^{j(\omega t - \beta_e S_1)}, \tag{19}$$

$$u = u_{10} \cos(\beta_\rho S_1)\, e^{j(\omega t - \beta_e S_1)}. \tag{20}$$

These expressions are returned to the form of sinusoids with a driving term equal to $u_{10} \sin\omega t$ by taking the imaginary parts of Equations (19) and (20), resulting in

$$i = AI_o \cos \omega t, \tag{21}$$

$$u = Bu_o \sin \omega t, \tag{22}$$

where

$$A = \frac{\beta_e}{\beta_\rho} \frac{u_{10}}{u_o} \sin(\beta_\rho S_1), \tag{23}$$

$$B = \frac{u_{10}}{u_o} \cos(\beta_\rho S_1). \tag{24}$$

Having defined the input conditions to the second gap in terms of constants and a parameter (the first-gap voltage) that can be related to power

input to the first gap, we can now assume a sinusoid of voltage at the second gap. In the case of an absence of drive at the middle cavity, this voltage will be simply that induced in the second gap by an a-c beam current. Where there is external drive at the second cavity, the gap voltage resulting from this external drive will add vectorially to the induced voltage. In either case the result is a voltage which can be specified in terms of its magnitude and phase angle, as

$$\overline{V}_2 = \left|V_2\right| \cos(\omega t + \phi) \quad , \tag{25}$$

where ϕ is the angle by which V_2 leads i at the center of the second gap. Newton's law is now applied to the motion of electrons in the second gap:

$$\dot{z} = \frac{e\left|V_2\right|}{md_2} \cos(\omega t + \phi) \quad . \tag{26}$$

Integrating this expression between the limits $t_2 - \frac{\theta_2}{2\omega}$ and $t_2 + \frac{\theta_2}{2\omega}$, where t_2 is time referred to the center of the gap, one obtains for exit velocity, the expression,

$$\dot{z} = \frac{e\left|V_2\right| M_2}{mu_o} \cos(\omega t_2 + \phi) \quad , \tag{27}$$

$$u_{exit} = u_o + u_1 + \dot{z} = u_o \left[1 + B \sin \omega t_2 + \cos(\omega t_2 + \phi)\right] \quad , \tag{28}$$

where

$$C = \frac{e\left|V_2\right| M_2}{mu_o^2} \quad . \tag{29}$$

A useful simplification results from combining terms in Equation (28)

so that

$$u_{exit} = u_o \left[1 + D \sin(\omega t_2 + \gamma)\right] , \tag{30}$$

where

$$D^2 = B^2 + C^2 - 2BC \cos \phi , \tag{31}$$

$$\gamma = \tan^{-1} \frac{C \cos \phi}{C \sin \phi - B} . \tag{32}$$

The length of the second drift space S_2 can be expressed as a product of exit velocity and time difference as follows:

$$S_2 = u_{exit} (t_3 - t_2) . \tag{33}$$

Solving Equation (33) for t_3 gives

$$t_3 = t_2 + \frac{S_2}{u_{exit}} \approx t_2 + \frac{S_2}{u_o} \left[1 - D \sin(\omega t_2 + \gamma)\right] . \tag{34}$$

The Fourier expansion of the a-c current density in the third gap can be expressed as

$$i_3 = \sum_{n=1}^{\infty} a_n \cos n\omega t_3 + b_n \sin n\omega t_3 , \tag{35}$$

where

$$a_n = \frac{1}{\pi} \int_{-\pi}^{\pi} i_3 \cos n\omega t_3 \, d(\omega t_3) , \tag{36}$$

$$b_n = \frac{1}{\pi} \int_{-\pi}^{\pi} i_3 \sin n\omega t_3 \, d(\omega t_3) \quad . \tag{37}$$

Substituting Equation (34) into (37) and making use of the equation of conservation of charge results in

$$i_3 \, dt_3 = i_2 \, dt_2 \quad ; \tag{38}$$

it then follows that

$$a_1 = \frac{1}{\pi} \int_{-\pi}^{\pi} I_o (1 + A \cos \omega t_2) \cos \left[\omega t_2 + \frac{\omega S_2}{u_o} - \frac{\omega S_2 D}{u_o} \sin (\omega t_2 + \gamma) \right] d\omega t_2 \quad , \tag{39}$$

$$b_1 = \frac{1}{\pi} \int_{-\pi}^{\pi} I_o (1 + A \cos \omega t_2) \sin \left[\omega t_2 + \frac{\omega S_2}{u_o} - \frac{\omega S_2 D}{u_o} \sin(\omega t_2 + \gamma) \right] d\omega t_2 \quad . \tag{40}$$

It should again be noted that the d-c current density, I_o, is a negative number as a result of the flow of conventional current from anode to cathode of the model.

Integrating Equations (39) and (40) by parts and making use of various Bessel function identities, it is possible to express the normalized a-c current in the third gap as

$$\left| \frac{I_3}{I_o} \right| = \left| 2 J_1 \left[\frac{\omega S_2 D}{u_o} \right] \cos \left(\omega t + \gamma - \frac{\omega S_2}{u_o} \right) \right.$$

$$\left. - A J_2 \left[\frac{\omega S_2 D}{u_o} \right] \cos \left(\omega t - \frac{\omega S_2}{u_o} \right) - A J_o \left[\frac{\omega S_2 D}{u_o} \right] \cos \left(\omega t + \delta\gamma - \frac{\omega S_2}{u_o} \right) \right| \quad , \tag{41}$$

where the J's indicate Bessel functions of the first kind, of orders 0,1,and 2.

It is worth noting that if the first-cavity drive is allowed to go to zero, the vanishing of the corresponding A term in Equation (41) causes the expression to reduce to a first-order Bessel function, while the model reduces to a two-cavity klystron consisting of the second and third cavities and the second drift space. This result is thus in accord with that of Webster[3] for the ballistic analysis of the two-cavity klystron.

Before examining the expression for the normalized output current of the three-cavity klystron further, a possible simplification should be examined. It will be noted that Equation (24) contains a multiplier, $\cos \beta_\rho S_1$. In a completely general model of a klystron, this term might be allowed to assume any value between -1 and 1. Variations in this term, however, will be accompanied by complementary variations in Equation (23), which has a multiplier, $\sin \beta_\rho S_1$. To maximize current output at the second gap and thus to maximize induced voltage in the second gap, it would be desirable to have term A_1, i.e., Equation (23), equal to unity. If this were the case, term B, i.e., Equation (24), would be equal to zero. This will be true if the length of the first drift space is one-quarter of a plasma wavelength. An investigation of the parameters of the SAS-61 klystron as operated in this experiment, assuming a beam diameter equal to the diameter of the grids in the middle cavity, shows the following:

$$V_o = 13 \text{ kv} ,$$

$$u_o = 6.76 \times 10^7 \text{ m/sec} ,$$

$$S_1 = 3.03 \times 10^{-2} \text{ m} ,$$

$$I_o = -3.18 \text{ a/m}^2 ,$$

$$\omega_\rho = 3.05 \times 10^9 \text{ radians/sec} ,$$

$$\beta_\rho S_1 = 1.37 = 78.5^\circ ,$$

$$\cos \beta_\rho S_1 = 0.199 .$$

Since the diameter of the grid in the second cavity is an upper bound for the beam diameter, the value calculated for I_o is a lower bound for the current density I_o. This indicates that the true value of $\cos \beta_\rho S_1$ is less than 0.199 and justifies neglecting it in the application of this model to the SAS-61 tube. This approximation would be further improved by applying a plasma-frequency reduction factor to ω_ρ. It then follows that

$$B = 0 , \quad D = C , \quad \gamma = \phi + \frac{\pi}{2} ; \qquad (42)$$

therefore,

$$\left|\frac{I_3}{I_o}\right| = \left| 2 J_1\left[\frac{\omega S_2 C}{u_o}\right] \cos\left(\omega t + \phi + \frac{\pi}{2} - \frac{\omega S_2}{u_o}\right) - A J_2\left[\frac{\omega S_2 C}{u_o}\right] \cos\left(\omega t - \frac{\omega S_2}{u_o}\right) - A J_o\left[\frac{\omega S_2 C}{u_o}\right] \cos\left(\omega t + 2\phi + \pi - \frac{\omega S_2}{u_o}\right)\right| . \qquad (43)$$

Substituting values for A and C, and shifting the time reference to eliminate the phase angle resulting from drift time in the second drift space gives

$$\left|\frac{I_3}{I_o}\right| = \left| -2 J_1\left[\frac{\omega S_2 M_2 |V_2|}{2 V_o}\right] \sin(\omega t + \phi) - \frac{\beta_e}{\beta_\rho} \frac{|V_1|}{2 V_o} J_2\left[\frac{\omega S_2 M_2 |V_2|}{2 V_o}\right] \cos \omega t + \frac{\beta_e}{\beta_\rho} \frac{|V_1|}{2 V_o} J_o\left[\frac{\omega S_2 M_2 |V_2|}{2 V_o}\right] \cos(\omega t + 2\phi)\right| . \qquad (44)$$

Equation (45) consists of a number of constants and three parameters, which are related to drive at the first and second cavities and to the tuning of the middle cavity. An additional parameter, the length of the final drift space, was fixed in this experiment, but it can be seen from Equation (45) to have the same effect upon output current as the magnitude of middle-cavity voltage. It is planned to evaluate this expression using both the parameters of the experiment and also the length of the final drift space, and to compare the results thus obtained with the experimental results.

CONCLUSIONS

It is apparent from this experiment that middle-cavity drive power has no effect upon the output of a three-cavity klystron above saturation that could not be achieved equally well or better by optimal uptuning of the middle cavity at a given level of first-cavity drive power. Inspection of any of the experimental curves shows that middle-cavity drive power in the most favorable phase reduces the output or produces a negligible change in the output when first-cavity drive power is at the optimum level. It can be seen that certain conditions produce an increase in output power which is greater than the amount of middle-cavity drive. This effect is most noticeable in the curve for a synchronously tuned middle cavity. With a first-cavity input of thirty watts, the application of one kilowatt at the middle cavity produced an increase in output power of 2.9 kilowatts. If the middle cavity is tuned up in frequency to produce a maximum power output at thirty watts input, however, output power increases to 7.6 kilowatts, as compared with the maximum output power of 6.2 kilowatts achieved with synchronous tuning and with one

kilowatt drive at the middle cavity. The same pattern is evident to a lesser degree in the other experimental curves. In no case does the application of power to the middle cavity produce more output above saturation than optimum uptuning of the middle cavity could produce without the use of any additional power.